

Transcription factor target site search and gene regulation in a background of unspecific binding sites

Authors

Johannes Hettich and J. Christof M. Gebhardt[#]

Institute of Biophysics, Ulm University, Albert-Einstein-Allee 11, 89081 Ulm, Germany

[#] corresponding author, email: christof.gebhardt@uni-ulm.de

Abstract

Response time and transcription level are vital parameters of gene regulation. They depend on how fast transcription factors (TFs) find and how efficient they occupy their specific target sites. It is well known that target site search is accelerated by TF binding to and sliding along unspecific DNA and that unspecific associations alter the occupation frequency of a gene. However, the relation between both parameters and whether they can be optimized simultaneously is mostly unclear. We developed a simple but general and powerful state-based formalism to calculate search times to target sites on and occupation frequencies of promoters of arbitrary state structure. To demonstrate our approach, we consider promoters activated by a single TF, by two coactivators or in the presence of a competitive inhibitor. We find that target site search time and promoter occupancy differentially vary with the unspecific dissociation rate constant. Both parameters can be harmonized by adjusting the specific dissociation rate constant of the TF. However, while measured DNA residence times of various eukaryotic TFs correspond to a fast search time, the occupation frequencies of target sites are generally low. Cells might tolerate low target site occupancies as they enable timely gene regulation in response to a changing environment.

Keywords

Facilitated diffusion, dimerization, competitive binding, master equation, multi-state model

Introduction

Gene regulation is mediated to large extend by transcription factors (TFs) interacting with specific target sites on DNA (1, 2). Frequently, TFs perform their regulatory function as homo- or heterodimers (3), for example nuclear receptors (4). Once bound, TFs recruit activating or repressing cofactors, chromatin remodelers and the transcription machinery (5). This recruiting activity and as a consequence the regulatory function of TFs is more efficient the larger their occupation frequency of the specific target site is (6, 7).

The time a TF needs to find its specific target site in part determines the response time of a gene. It has been proposed that the TF target site search is accelerated if the TF not only tests individual sites on DNA by freely diffusing through the nucleoplasm (3D search), but in addition slides along DNA in an unspecific binding mode (1D search)(8, 9). Indeed, binding of proteins to and sliding along unspecific DNA sequences is a common observation (10-15). How various parameters such as the ratio of 1D to 3D search mechanisms, crowding, roadblocks or DNA conformation influence the search time has been investigated comprehensively (8, 16-25). It is also known that unspecific binding alters the occupation frequency of a gene (16, 17, 26, 27). Yet it is unclear how both parameters compare under variation of TF-DNA dissociation rate constants. How do TFs distribute over time between their specific target site and the myriad of unspecific sites on DNA (Figure 1)? May a TF find its target site quickly while at the same time occupying it efficiently to optimize gene regulation, or are both requirements contradictory?

To answer these questions, we developed a simplified but powerful state-based formalism including gene promoters of arbitrary state structure. TF target site search times are obtained accurately by solving the Kolmogorov equations for the time evolution to the steady state, and occupation frequencies by considering the steady state distribution. We applied our approach to a simple promoter activated by a single TF and validated our results by comparison with a microscopic search model (23, 28). Next, we expanded the activation mechanism by adding a cofactor dimerizing on DNA or a competitor inhibiting specific binding of the TF. We found that both fast target site search and high occupation frequency can be harmonized by adjusting the binding time to the specific target site. Notably, experimentally obtained unspecific and specific dissociation rate constants of various TFs indicate that many TFs indeed are optimized for fast target site search, but not for high occupation frequencies of this site. Activating or competing cofactors allow modulating the optimal conditions, enabling the cell to fine tune the response times and activities of genes in genetic networks.

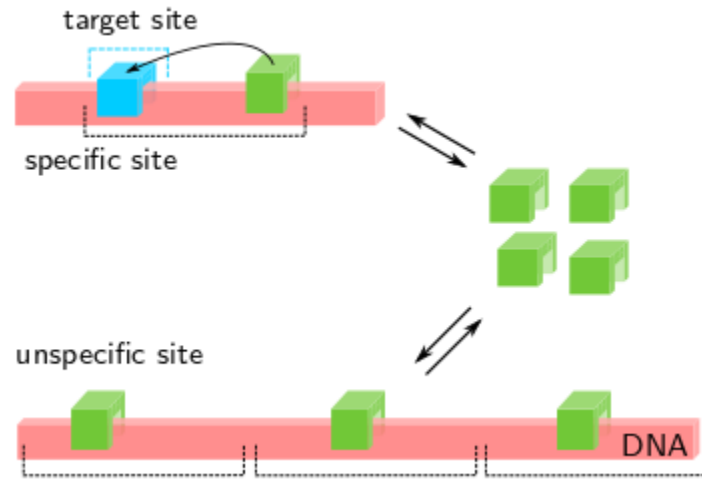


Figure 1: General scheme of a genetic network. A specific binding site (promoter) of arbitrary state structure is embedded in a pool of unspecific binding sites. Drawn is a simple promoter consisting of the target site and surrounding unspecific DNA sequences. Depending on the respective binding times, the TF distributes between the nucleoplasm, unspecific sites and the promoter. If unspecific binding is favored, both the search time and promoter occupancy decrease.

Materials and Methods

1. Mean number of free TFs

Single TF

The unspecific binding of the TF crowd is modelled by a chemical reaction scheme in which the rates depend on the number of bound TFs and occupied binding sites (29). Let the total number of unspecific binding sites be B . We assume that one binding site BS can only contain one TF at a time. The chemical reaction for binding to unspecific sites is



If l TFs are bound to DNA, each TF can dissociate independently with the dissociation rate constant μ_1 . The association rate constant of TFs is given by the product of free TFs $N-l$, the free binding sites $B-l$ and the diffusion limited arrival rate λ_{10} . The stationary Kolmogorov equation for the probability p_l to find l bound TF is

$$0 = \mu_1((l+1)p_{l+1} - p_l) - \lambda_{10}((N-l)(B-l)p_l - (N-l+1)(B-l+1)p_{l-1}) \quad 2$$

where $p_l = 0$ for $l < 0 \cup l > M = \min(N, B)$

This is a recursion which can be solved for p_l .

$$Z = p_0^{-1} = \sum_{l=0}^M \binom{N}{l} \binom{B}{l} l! K_0^l \quad \text{where } K_0 = \frac{\lambda_{10}}{\mu_1} \quad 3$$

The expectation value \bar{n} of unspecifically bound TFs is obtained by the derivative

$$\bar{n} = K_0 \frac{d}{d K_0} \ln(Z) \quad 4$$

In order to find an approximation for this equation, we take the average over Eq. 2 by multiplying with l and summing up and obtain

$$\frac{\mu_1}{\lambda_{10}} \bar{n} = BN - (B+N)\bar{n} + \bar{n}^2 \quad 5$$

For $B \gg N$ the approximation

$$\bar{n}(\mu_1) = \frac{N}{1 + \frac{\mu_1}{\lambda_{10} B}} \quad 6$$

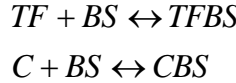
is obtained. This yields the free number of TFs

$$n_f(\mu_1) = \frac{N}{1 + \frac{\lambda_{10}B}{\mu_1}}$$

7

TF and competitor

If a second species C is present its binding to unspecific sites does not happen independently from the unspecific binding of the TF. Therefore, this case has to be accounted for. We again assume that a binding site can only be occupied by one molecule. The binding can be written in terms of the chemical reaction



8

The stationary Kolmogorov equation is

$$\begin{aligned} 0 &= \mu_1((l_1+1)p_{l_1+1,l_2} - p_{l_1,l_2}) \\ &- \lambda_{10}((N_1 - l_1)(B - l_1 - l_2)p_{l_1,l_2} - (N_1 - l_1 + 1)(B - l_1 - l_2 + 1)p_{l_1-1,l_2}) \\ &- \zeta_1((l_2+1)p_{l_1,l_2+1} - p_{l_1,l_2}) \\ &- \Lambda_{10}((N_2 - l_2)(B - l_1 - l_2)p_{l_1,l_2} - (N_2 - l_2 + 1)(B - l_1 - l_2 + 1)p_{l_1,l_2-1}) \\ \text{where } p_{l_1,l_2} &= 0 \text{ for } l_1, l_2 < 0 \cup l_1 > M_1 = \min(N_1, B), l_2 > M_2 = \min(N_2, B) \end{aligned} \quad 9$$

9

This is a recursion which can be solved for p.

$$Z = p_0^{-1} = \sum_{l_1, l_2=0}^{M_1, M_2} \binom{N_1}{l_1} \binom{N_2}{l_2} \binom{B}{l_1 + l_2} (l_1 + l_2)! K^{l_1} H^{l_2} \quad 10$$

where $K = \lambda_{10}/\mu_1$ and $H = \Lambda_{10}/\zeta_1$. The expectation values \bar{n}_1, \bar{n}_2 of unspecifically bound TF and competitor are obtained by the derivatives

$$\begin{aligned} \bar{n}_1 &= K \frac{d}{dK} \ln(Z) \\ \bar{n}_2 &= H \frac{d}{dH} \ln(Z) \end{aligned} \quad 11$$

We obtain two equations by averaging over l_1 and l_2

$$\begin{aligned} \frac{\mu_1}{\lambda_{10}} \bar{n}_1 &= BN_1 - B\bar{n}_1 - N_1(\bar{n}_1 + \bar{n}_2) + \overline{\bar{n}_1(\bar{n}_1 + \bar{n}_2)} \\ \frac{\zeta_1}{\Lambda_{10}} \bar{n}_2 &= BN_2 - B\bar{n}_2 - N_2(\bar{n}_1 + \bar{n}_2) + \overline{\bar{n}_2(\bar{n}_1 + \bar{n}_2)} \end{aligned} \quad 12$$

For $B \gg N_1, N_2$ we obtain

$$\bar{n}_1 = \frac{N_1}{1 + \frac{\mu_1}{\lambda_{10}B}} \quad \bar{n}_2 = \frac{N_2}{1 + \frac{\zeta_1}{\Lambda_{10}B}} \quad 13$$

This yields the mean free number of TFs and of the second species

$$n_{1,f} = \frac{N_1}{1 + \frac{\lambda_{10}B}{\mu_1}} \quad n_{2,f} = \frac{N_2}{1 + \frac{\Lambda_{10}B}{\zeta_1}} \quad 14$$

2. General formula for the search time and the occupation frequency of specific target sites

We use a multistate model in order to model specific binding sites. On these sites two effects can occur: unspecific binding and specific binding to the target site. In addition, the specific site can be empty with respect to the TF. Let the total number of states of the specific site be L. We introduce three index sets

$$E = \{e_1, e_2, \dots\} \quad D = \{d_1, d_2, \dots\} \quad G = \{g_1, g_2, \dots\} \quad 15$$

E contains states in which no TF is bound, D contains states in which TFs are bound but the gene is not activated and G contains states in which TFs are bound and the gene is activated. The transition matrix T contains the transition rate constants between the states. The time evolution of the system is described with the Kolmogorov equation for the binding probabilities p

$$\dot{\vec{p}} = \mathbf{T}\vec{p} \quad 16$$

The sum over all probabilities is normalized to 1.

We now calculate the target site search time. We define the search time as the time until any TF of the crowd binds to the target site. Since we are interested in the first binding event we set all outgoing transition of G to zero and thereby obtain the matrix \mathbf{U} . Next, we consider the flux of probabilities leaving the sets E,D

$$f = -\frac{d}{dt} \sum_{E \cup D} p_i \quad 17$$

In order to obtain this flux we need to solve the Cauchy problem of the Kolmogorov equations

$$\dot{\vec{p}} = \mathbf{U}\vec{p} \quad p_i = 0 \quad \forall i \in D \cup G \quad p_i = p_{0,i} \quad \forall i \in E \quad 18$$

These initial conditions represent an empty specific site and therefore cover the whole target search which consists of 3D diffusion and transition to the target site from the unspecifically bound state. The flux is the distribution of search times (30). The expectation value of this distribution is obtained by

$$\tau = \int_0^\infty f(t)t dt = \int_0^\infty -t \frac{d}{dt} \sum_{E \cup D} p_i dt \quad 19$$

By partial integration we obtain

$$\tau = \left[t \sum_{E \cup D} p_i \right]_0^\infty + \int_0^\infty \sum_{E \cup D} p_i dt = \sum_{E \cup D} Q_i \quad 20$$

where

$$Q_i = \int_0^\infty p_i dt \quad 21$$

Thus, the mean search time can be calculated by the integral over time of the probabilities. These can be obtained by integration over both sides of Eq. 16 which yields

$$\vec{p}(\infty) - \vec{p}(0) = \mathbf{U} \vec{Q} \quad 22$$

We now calculate the occupation frequency by solving the steady state Kolmogorov equation

$$0 = \mathbf{T} \vec{p} \quad 23$$

for p . We obtain the occupation frequency by summing over all target states G .

Promoter activated by a single TF

The transition matrix of the three-state model is

$$\mathbf{T} = \begin{pmatrix} -\lambda - \lambda_1 & \mu_1 & \mu \\ \lambda_1 & -\mu_1 - \lambda_2 & \mu_2 \\ \lambda & \lambda_2 & -\mu - \mu_2 \end{pmatrix} \quad 24$$

The states are divided into the sets

$$E = \{1\} \quad D = \{2\} \quad G = \{3\} \quad 25$$

By solving Eq. 23 for p_3 we obtain the occupation frequency

$$p = \left[1 + \frac{m}{l} \left(1 + \frac{l_1}{m_1} \right) \right]^{-1} \quad 26$$

By setting transitions that leave the target states to zero we obtain

$$\mathbf{U} = \begin{pmatrix} -\lambda - \lambda_1 & \mu_1 & 0 \\ \lambda_1 & -\mu_1 - \lambda_2 & 0 \\ \lambda & \lambda_2 & 0 \end{pmatrix} \quad 27$$

By using Eq. 22 and the initial conditions

$$\vec{p}(\infty) = (0,0,1) \quad \vec{p}(0) = (1,0,0) \quad 28$$

we obtain the target site search time

$$t = \frac{I_1 + I_2 + M_1}{k} \quad \text{where} \quad k = I_2 + M_1 + \frac{I_1 I_2}{I} \quad 29$$

Promoter activated by two coactivating TFs

We assume that both TFs independently bind to two specific target sites with similar rate constants. We further assume that unspecific and specific states can be occupied by two cofactors at the same time. The states are divided into the sets

$$E = \{1\} \quad D = \{2,3,4,5\} \quad G = \{6\} \quad 30$$

The transition matrix of the model for the competitor (see Figure 2) is

$$\mathbf{U} = \begin{pmatrix} -d_1 & \mu_1 & \mu & 0 & 0 & 0 \\ \lambda_1 & -d_2 & \mu_2 & 2\mu_1 & \mu & 0 \\ \lambda & \lambda_2 & -d_3 & 0 & \mu_1 & 0 \\ 0 & \lambda_1 & 0 & -d_4 & \mu_2 & 0 \\ 0 & \lambda & \lambda_1 & 2\lambda_2 & -d_5 & 0 \\ 0 & 0 & \lambda & 0 & \lambda_2 & 0 \end{pmatrix} \quad 31$$

$$d_1 = \lambda_1 + \lambda$$

$$d_2 = \lambda_1 + \lambda_2 + \lambda + \mu_1$$

$$d_3 = \lambda_1 + \lambda + \mu + \mu_2$$

$$d_4 = 2\lambda_2 + 2\mu_1$$

$$d_5 = \lambda_2 + \mu_1 + \mu_2 + \mu$$

The probability for the target site to be occupied is calculated by the detailed balance

$$p = p_6 = \frac{K^2}{1 + (1 + K + K_1)^2} \quad 32$$

with equilibrium constants from Figure 2. We calculated the search time by numerically solving the system of equations Eq. 31.

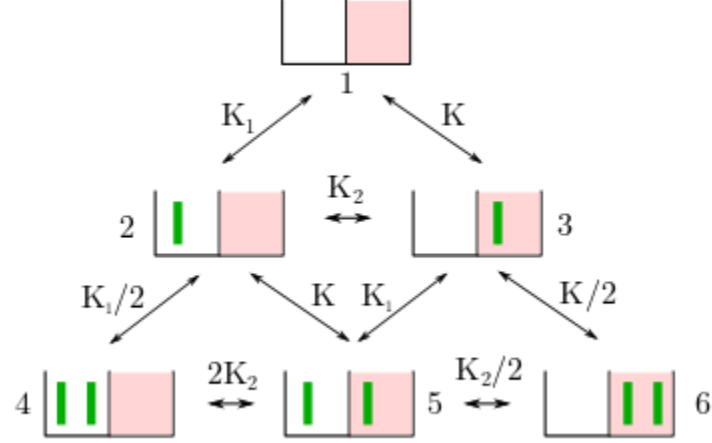


Figure 2: Six-state model of a binding site that is active if two cofactors are specifically bound. Unspecific and target states can contain two monomers at the same time. The equilibrium constants are written in terms of the ratios *bind/unbind* with the rates $K_i = \lambda_i/\mu_i$ $i=1,2$. The direct arrival at the target site with 3D diffusion of the protein is $K = \lambda/\mu$

Promoter activated by a single TF subject to inhibitory competition

The competitor is assumed to inhibit binding sites of the TF. Since the unspecific and target states can be empty or contain either a competitor or a TF we obtain nine states. These states are divided into the sets

$$E = \{1\} \quad D = \{2,3,4,6,7\} \quad G = \{5,8,9\} \quad 33$$

The transition matrix of the model for the competitor (see Figure 3) is

$$\mathbf{U} = \begin{pmatrix} -d_1 & \zeta & \zeta_1 & \mu_1 & 0 & 0 \\ \Lambda & -d_2 & \Lambda_2 & 0 & \zeta_1 & \mu_1 \\ \Lambda_1 & \zeta_2 & -d_3 & 0 & \zeta & 0 \\ \lambda_1 & 0 & 0 & -d_4 & 0 & \zeta \\ 0 & \Lambda_1 & \Lambda & 0 & -d_6 & 0 \\ 0 & \lambda_1 & 0 & \Lambda & 0 & -d_7 \end{pmatrix} \quad 34$$

$$d_1 = \lambda_1 + \lambda + \Lambda_1 + \Lambda$$

$$d_2 = \lambda_1 + \Lambda_1 + \zeta_2 + \zeta$$

$$d_3 = \zeta_1 + \Lambda_2 + \Lambda + \lambda$$

$$d_4 = \mu_1 + \lambda + \Lambda + \lambda_2$$

$$d_6 = \zeta_1 + \zeta$$

$$d_7 = \mu_1 + \zeta$$

For simplicity we did not include the target states. The probability for the target site to be occupied is calculated using detailed balance

$$p = p_5 + p_8 + p_9 = \frac{1}{1 + K^{-1}(1 + H)}$$

35

with equilibrium constants from Figure 3. The search time is calculated by numerical matrix inversion of \mathbf{U} .

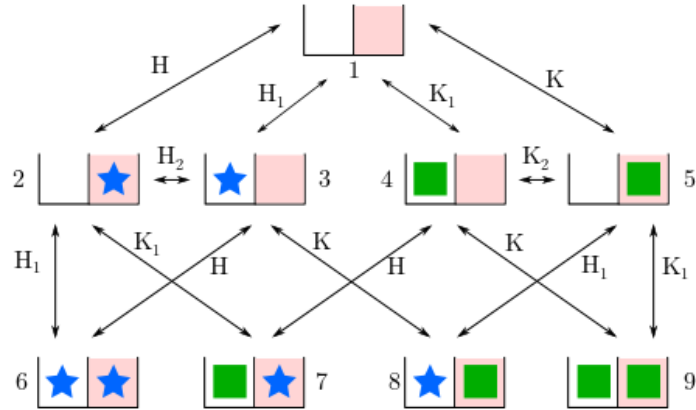


Figure 3: Nine state model of the specific binding site with competitor. It is assumed that one protein can perform 1D diffusion on the specific binding site and that there is one specific target site. The competitor and the protein of interest occupy these states exclusively. Since a site can have three states, empty, competitor or protein bound, there are $3^2 = 9$ states of the specific binding site. The equilibrium constants are written in terms of the ratios *bind/unbind* with the rates $K_i = \lambda_i/\mu_i$; $H_i = \Lambda_i/\zeta_i$ $i=1,2$. The equilibrium constants H_2, K_2 are chosen such that the law of detailed balance is fulfilled. The direct arrival at the target site with 3D diffusion of the protein is $K = \lambda/\mu$ for the TF and $H = \Lambda/\zeta$ for the competitor.

3. Model for target site search by explicit 1D diffusion

We here model the TF target site search by explicitly accounting for 1D diffusion events on unspecific DNA, interrupted by 3D diffusion until the specific target site is found (16, 17, 19-25, 28, 33, 49) (Figure 4). The association rate constant to any base pair is λ_0 . We model the sliding of the TF by single base pair sliding steps with transition rate constant α and an average sliding time of μr^{-1} . The transcription factor has one consensus DNA sequence to which it can bind specifically. As in (20, 23), we include static roadblock molecules (crowders) in our model.

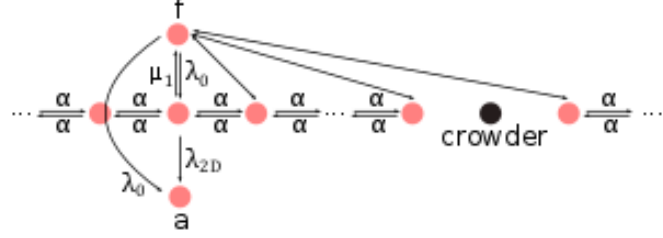


Figure 4: Model for TF target site search explicitly accounting for 1D and 3D diffusion. State f corresponds to the free TF. State a corresponds to the TF bound to its specific target site. The TF may arrive at any base pair of the genome by 3D diffusion and slides along unspecific DNA with sliding rate constant α . If bound unspecifically to the target site the TF may switch to the specific binding mode with transition rate constant λ_0 . The TF may also arrive in the specifically bound conformation directly after 3D diffusion. We accounted for crowding by periodically blocking sliding transitions between two sites every M base pairs. With R crowders the total genome length thus is $L=R \cdot M$.

We calculated the target site search time by applying our formalism of Materials and Methods, Section 2, to the initial value problem

$$E = \{f\} \quad D = \{-n, \dots, n\} \quad G = \{a\} \quad 36$$

This leads to the result

$$\begin{aligned} \tau &= \left(\frac{1}{\lambda_0} + \frac{L}{\mu_1} \right) \cdot \frac{r}{1+r} \\ r &= \frac{\mu_1}{\lambda_{2D}} + \frac{1+q^M}{1+q} \cdot \frac{1-q}{1-q^M} \\ q &= 1 + \frac{\mu_1}{2\alpha} - \sqrt{\left(1 + \frac{\mu_1}{2\alpha} \right)^2 - 1} \end{aligned} \quad 37$$

In order to find the sliding rate constant α between base pairs, we treat the continuous diffusion case $\mu_1 \rightarrow 0$ without crowding,

$$\tau = \left(\frac{1}{\lambda_0} + \frac{L}{\mu_1} \right) \cdot \frac{1}{2\sqrt{\alpha/\mu_1}} \quad 38$$

We compared this result to the formula

$$\tau = \left(\frac{1}{\lambda_0 L} + \frac{1}{\mu_1} \right) \cdot \frac{L}{n_D} \quad \text{where} \quad n_D = \frac{2}{l_{bp}} \sqrt{\frac{D}{\mu_1}} \quad 39$$

derived by (28) which includes the 1D diffusion constant D measured experimentally in (12, 13, 31). The number n_D is the number of visited base pairs per sliding event. Both equations yield the same results if we set

$$n_D = 2\sqrt{\frac{\alpha}{\mu_1}} = \frac{2}{l_{bp}}\sqrt{\frac{D}{\mu_1}} \quad 40$$

This result enables us to obtain the sliding rate constant α

$$\alpha = \frac{D}{l_{bp}^2} \quad 41$$

Using $D=0.01 \mu\text{m}^2\text{s}^{-2}$ and $l_{bp}=0.34 \text{ nm}$ we obtain $\alpha=8.7 \cdot 10^4 \text{ s}^{-1}$. In Figure 3, this Diffusion model is plotted using $N=100$, $B=10^4$ and $\lambda_0=10^{-5} \text{ s}^{-1}$. The rate for transition to specific binding on the target site $\lambda_{2D}=160 \text{ s}^{-1}$ was chosen such that the curves of the Diffusion model agree with the new model of Eq. 45.

Results

Target site search time and occupation frequency of a gene

Besides binding to their specific target site, TFs have an, albeit lower, affinity to any sequence on DNA which gives rise to unspecific associations (1, 32). We thus considered a promoter embedded in a pool of unspecific binding sites (Figure 1) and translated this setting into a system of states with decoupled unspecific and specific sites (Figure 5). We solved the Kolmogorov equations to obtain target site search times and occupation frequencies to three different promoter structures, a simple promoter bound by a single activating TF, a promoter activated by two independently binding TFs with similar kinetic rate constants and a promoter to which an additional inhibitory binding competitor can bind.

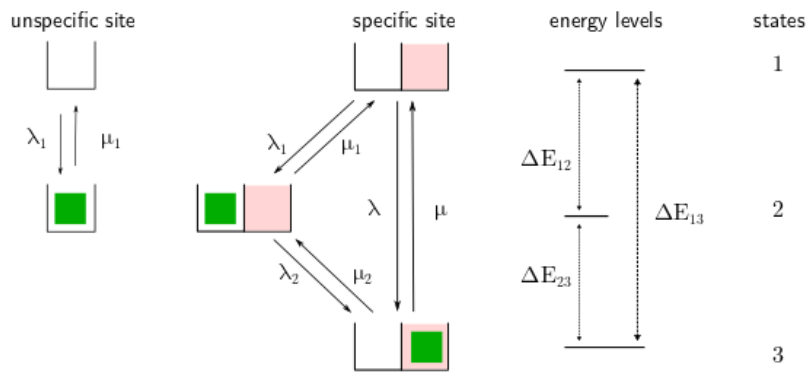


Figure 5: Three state model of a genetic network consisting of a promoter with a specific target site for a single TF and unspecific sequences. The first state denotes free TFs, the second state denotes unspecifically bound TFs and the third state denotes TFs bound to the specific target site. We ascribe each state an energy level, energy differences are connected to the respective ratio of on- and off-rate constants by the law of detailed balance.

Promoter activated by a single TF

The simple promoter comprises the specific target site of the TF and surrounding unspecific DNA. Translated into our state-based formalism, the TF on the specific site has three states, free, unspecifically bound and bound to the specific target site (Figure 5). In our model, the TF can bind to its target site on the promoter either directly via 3D diffusion with association rate constant λ , or by first binding to the surrounding unspecific DNA with association rate constant λ_1 and a subsequent transition with rate constant λ_2 . λ_2 is a cumulative rate including a potential conformational change associated with binding to the target site (17) and a finite probability to find the target site when sliding on nearby unspecific sequences (15). The promoter is embedded in a background of B unspecific binding sites from which no direct transition to the target site can occur (Figure 5). For the size of unspecific sites we chose a fixed number of 40 bp, corresponding to experimental findings (14, 15). In vivo, the size of unspecific sites is limited by the presence of other DNA-bound molecules, not by the time a TF spends sliding on accessible DNA (20, 23), justifying a fixed size independent of μ_1 .

The association rate constants to unspecific or specific sites depend on the number of free TFs, n_f , which in turn depends on the unspecific dissociation rate constant according to

$$I_1(m_1) = n_f(m_1) / \lambda_{10} \quad I(m_1) = n_f(m_1) / \lambda_0 \quad 42$$

Here, we neglect a dependence on the dissociation rate constant of the target site since only one such site exists, which is not occupied during target site search. λ_0 and λ_{10} denote the diffusion limited arrival rate constants.

Association rate constants and dissociation rate constants are coupled by the law of detailed balance

$$\frac{I_{10}}{m_1} \times \frac{I_2}{m_2} = \frac{I_0}{m} \quad 43$$

We first calculated the number of free TFs n_f . If the total number of TFs N is much smaller than B , we find for n_f

$$n_f(\mu_1) = \frac{N}{1 + \frac{\lambda_{10}B}{\mu_1}} \quad 44$$

(Material and Methods, Section 1). For the following discussion we used the exact result for n_f derived in Materials and Methods, Section 1 and evaluated it numerically.

Next, we calculated the target site search time τ of the gene. We assumed an equilibrium distribution of free and unspecifically bound TFs given an unoccupied promoter and used the Kolmogorov equations to calculate the time until the first TF bound the target site (Materials and Methods, Section 2). Using the number of free TFs, we found for the target site search time (Figure 6)

$$t = \frac{I_1 + I_2 + m_1}{k} \quad \text{where} \quad k = I_2 + m_1 + \frac{I_1 / I}{\lambda_0} \quad 45$$

The search time exhibits a minimum corresponding to an optimally fast target search process, as for small μ_1 TFs are drawn towards unspecific DNA and the free pool of searching TFs becomes minimal while for large μ_1 the benefit of 1D diffusional scanning of DNA is negligible. This result is consistent with previous studies of the TF target site search problem (8, 9, 28, 33).

To validate our simplified calculation of the target site search time, we compared our result with the one from a microscopic model explicitly treating 1D diffusion in presence of static roadblocks limiting the sliding distance of TFs (20, 23) (Figure 6 and Materials and Methods Section 3, Figure 4). Both models agree very well. Since our simplified state based approach allows for straightforward incorporation of more complex promoter structures, we used it hereafter.

We calculated the occupation frequency p of the gene by eliminating λ_2 / μ_2 with Eq. 43 and solved the Kolmogorov equations (Materials and Methods, Section 2). We found for the occupation frequency (Figure 7)

$$p = \left[1 + \frac{m}{l} \left(1 + \frac{l}{m} \right) \right]^{-1}$$

46

This parameter increases monotonically with μ_1 and asymptotically approaches a maximum determined by the equilibrium constant of specific binding, since μ_1 directly determines the association rate constant to specific target sites (Eq. 42).

Promoter activated by two coactivating TFs

To model gene activation by two independently binding TFs of similar type, the promoter comprises two specific target sites, one for each TF, surrounded by unspecific DNA. Both TFs are assumed to bind independently with similar rate constants but activate the gene only if bound specifically at the same time as homo- or heterodimers. Translated into our state-based formalism, the TFs on the specific site have six states (Materials and Methods Section 2, Figure 2). We deliberately omitted binding interactions between both TFs (34), to focus on the contributions of DNA binding to target site search and occupation frequency and preserve the comparison to a single TF.

To calculate the target site search time of the promoter activated by two TFs, we solved the Kolmogorov equations of the dimeric system numerically (Figure 6 and Materials and Methods, Section 2). For the occupation frequency, we compared dimerization exclusively on DNA, as before, with dimerization already in solution (Figure 7).

Promoter activated by a single TF subject to inhibitory competition

To model gene activation in the presence of an inhibitory binding competitor, we introduced a second species that is able to bind to the same binding sites as the TF, but with own dissociation rate constants. Once occupied by the competitor, a binding site is sterically blocked for binding of the TF. Translated into our state-based formalism, the system has nine states (Materials and Methods Section 2, Figure 3).

We again numerically solved the Kolmogorov equations of the system with binding competitor to obtain the target site search time of the gene. The target site search time of the TF increases significantly if the unspecific dissociation rate constant ζ_1 of the competitor increases (Figure 8a). In this case more competitor is available to block the target site. Consequently, the occupation frequency of the gene drops under these conditions (Figure 8b). If the occupation of the specific target site by the competitor is modulated with the specific dissociation rate constant ζ of the competitor, a small value for ζ , i.e. a high occupation, leads to a similar effect (Figure 8c and d).

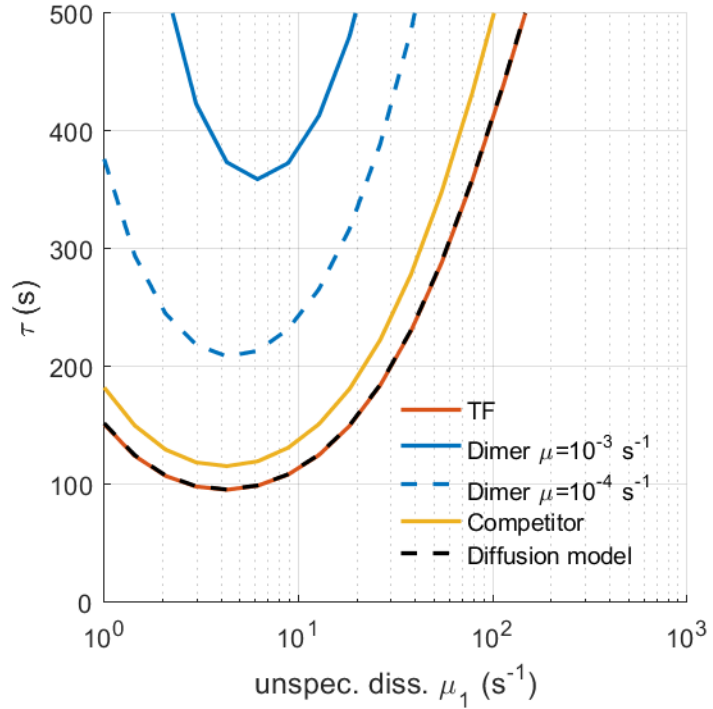


Figure 6: Comparison of the target site search time τ of the gene as function of the unspecific dissociation rate constant μ_1 between a promoter activated by a single TF (TF, red line), a promoter activated by a dimer ($\mu=10^{-3} \text{ s}^{-1}$, solid blue line), activated by a dimer with lower specific dissociation rate constant ($\mu=10^{-4} \text{ s}^{-1}$, dashed blue line) and when an inhibitory competitor of the TF is present (Competitor, yellow line). In addition, the TF target site search time calculated from a model explicitly accounting for 1D diffusion is indicated (Diffusion model, dashed black line). Simulation parameters are: $N=100$, $C=100$, $B=10^4$, $\lambda_{10}=\Lambda_{10}=4 \cdot 10^{-4} \text{ s}^{-1}$, $\lambda_0=\Lambda_0=10^{-5} \text{ s}^{-1}$, $\lambda_2=\Lambda_2=4 \text{ s}^{-1}$, $\zeta_1=1 \text{ s}^{-1}$, $\zeta=10^{-3} \text{ s}^{-1}$.

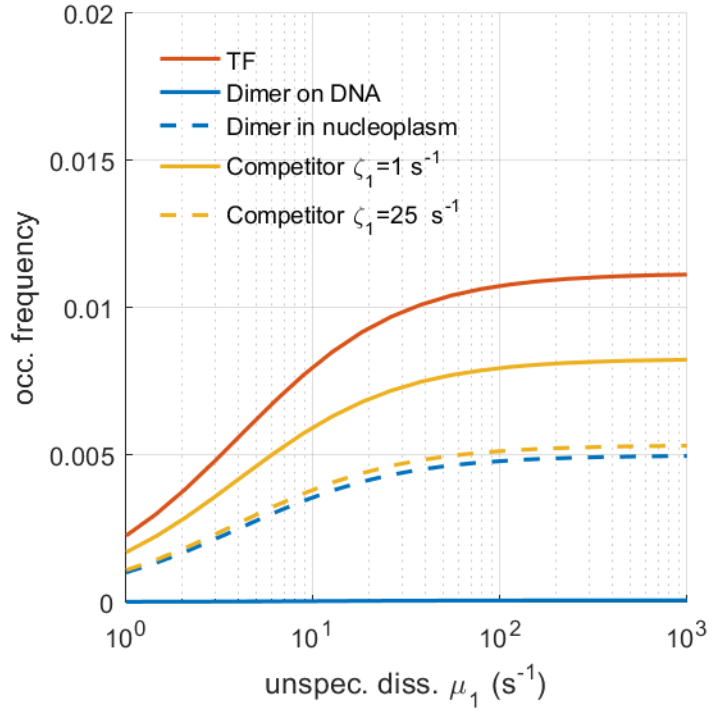


Figure 7: Comparison of occupation frequency p as function of the unspecific dissociation rate constant μ_1 between a promoter activated by a single TF (TF, red line), a promoter activated by a dimer formed on DNA (Dimer on DNA, blue line) and by a dimer formed in the nucleoplasm (Dimer in nucleoplasm, dashed blue line), when an inhibitory competitor of the TF is present (Competitor $\zeta_1=1\text{ s}^{-1}$, yellow line) and when the competitor has a larger unspecific dissociation rate constant (Competitor $\zeta_1=25\text{ s}^{-1}$, dashed yellow line). Simulation parameters are: $N=100$, $C=100$, $B=10^4$, $\lambda_{10}=\Lambda_{10}=4\cdot10^{-4}\text{ s}^{-1}$, $\lambda_0=\Lambda_0=10^{-5}\text{ s}^{-1}$, $\lambda_2=\Lambda_2=4\text{ s}^{-1}$, $\mu=10^{-1}\text{ s}^{-1}$, $\zeta=10^{-3}\text{ s}^{-1}$.

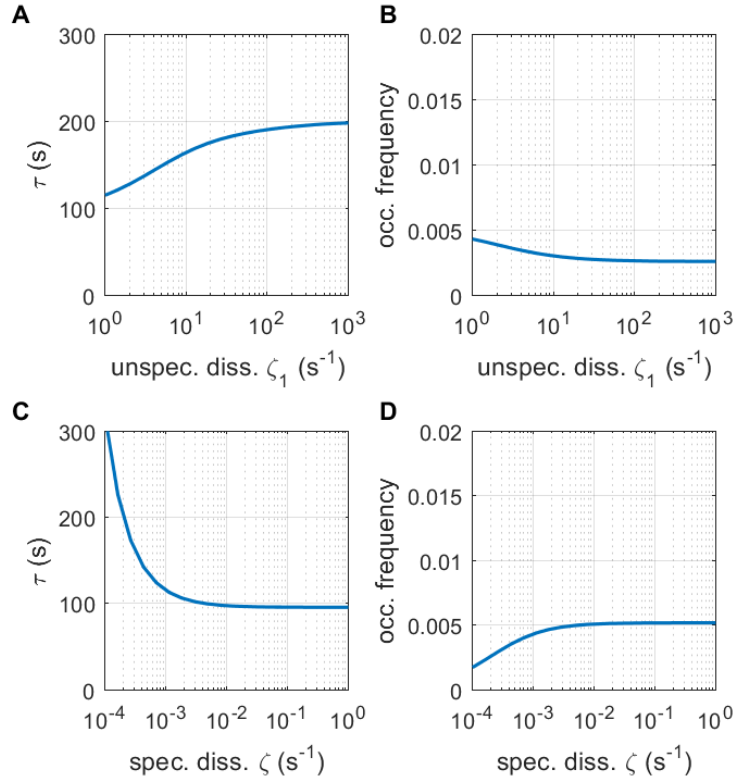


Figure 8: Influence of an inhibitory binding competitor. (A) Target site search time τ of the gene and (B) probability of the promoter to be occupied by a TF, p , as function of the unspecific dissociation rate constant ζ_1 of the competitor. (C) τ and (D) p as function of the specific dissociation rate constant ζ of the competitor. Simulation parameters are: $N=100$, $C=100$, $B=10^4$, $\lambda_{10}=\Lambda_{10}=4 \cdot 10^{-4}$ s⁻¹, $\lambda_0=\Lambda_0=10^{-5}$ s⁻¹, $\lambda_2=\Lambda_2=4$ s⁻¹, $\mu=10^{-1}$ s⁻¹, $\zeta=10^{-3}$ s⁻¹.

TFs are optimized for fast target site search but not for high occupation frequency

Since both target site search time and occupation frequency depend on μ_1 , we tested whether they assumed their respective optima, fast target site search and high occupation frequency, at similar values of the unspecific dissociation rate constant (Figure 9). To compare both quantities, we chose parameter values according to the physiological conditions in an eukaryotic cell. We varied the unspecific dissociation rate constant μ_1 in the interval 10^0 s $^{-1}$ to 10^3 s $^{-1}$ (12, 35-37) and the specific dissociation rate constant μ from 10^0 s $^{-1}$ to 10^{-4} s $^{-1}$ (36, 38-44). The arrival rate constant is given by the 3D diffusion limit under physiological salt concentrations, $\lambda_0=10^6$ (Ms) $^{-1}$ (28), which results in $\lambda_0=10^{-5}$ s $^{-1}$ in a typical cell volume of $100\mu\text{m}^3$. The arrival rate constant to the unspecific site scales with the size of unspecific sites of 40bp to $\lambda_{10}=4\cdot10^{-4}$ s $^{-1}$. We adjusted the transition rate constant $\lambda_2=4$ s $^{-1}$ in accordance with a low probability to bind the specific target site when scanning nearby unspecific DNA (15). In this case the rate limiting step of specific DNA-binding is the 3D diffusion to the specific site. Finally, we assumed that the promoter is embedded in a background of $4\cdot10^5$ bp of unspecific DNA, resulting in $B=10^4$ unspecific binding sites. This value revealed a fraction of DNA-associated TFs of 20%-40% reported by experiments (39-41). We found that a common optimum of target site search time and occupation frequency is only achieved for large unspecific and small specific dissociation rate constants (Figure 9).

We next compared our results to various eukaryotic TFs. We calculated their occupation frequencies using published values of unspecific and specific dissociation rate constants measured *in vivo*, and plotted these onto the theoretically derived occupation frequency (Figure 9 and Table 1). To be able to compare the TFs, we assumed that dimeric TFs such as GR already dimerized in solution, and considered a ratio of 100 TFs per specific target site, which is a good approximation for many eukaryotic TFs binding to hundreds of specific target sequences (45).

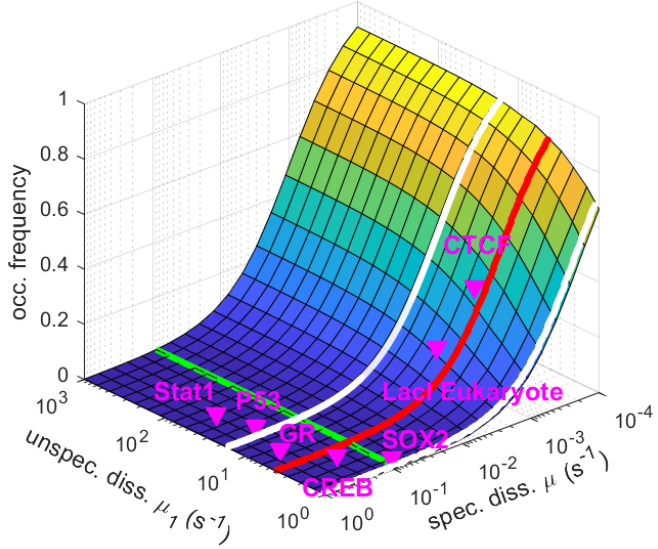


Figure 9: Occupation frequency p of the promoter by a TF as function of the unspecific (μ_1) and the specific (μ) dissociation rate constants. The values μ_1 of minimal (red line) and 1.5 times the minimal target site search time (white lines) are indicated. The green line at $\mu=10^{-1} \text{ s}^{-1}$ indicates the projection of the occupation frequency displayed in Figure 7. Symbols correspond to occupation frequencies of various TFs calculated from unspecific and specific dissociation rate constants measured by fluorescence microscopy in live cells. Simulation parameters are: $N=100$, $B=10^4$, $\lambda_{10}=4 \cdot 10^{-4} \text{ s}^{-1}$, $\lambda_0=10^{-5} \text{ s}^{-1}$, $\lambda_2=4 \text{ s}^{-1}$.

TF	$\mu_1 (\text{s}^{-1})$	$\mu (\text{s}^{-1})$	source
SOX2	1.3	0.08	(41)
LacI (mammalian cell)	5.6	0.003	(36, 42)
CREB	2.7	0.2	(43)
P53	20	0.3	(39)
Stat1	50	0.4	(38)
GR	6.7	0.5	(40, 46)
CTCF	5	0.001	(44)

Table 1: Unspecific and specific dissociation rate constants of transcription factors measured in live cells.

Discussion

We have introduced a simplified treatment of TF target site search by mathematically decoupling unspecific from specific binding and replacing explicit 1D diffusion with the dissociation rate constant from unspecific sites. We have shown that this replacement is able to model the search process in presence of static roadblock molecules to good approximation. While coarse-graining some of the microscopic details, the benefit of our approach is that it modularizes the discussion of promoter structures at the specific site and unspecific binding and therefore can offer a detailed insight into the dependencies of target site search time and occupation frequency on microscopic association and dissociation rate constants. Our model can be extended to include the geometry of DNA and crowding in the nucleoplasm (18, 47, 48), by changing the arrival and dissociation rate constants. In particular, protein-protein interactions could easily be incorporated using additional states.

The non-monotone dependency of the target site search time on the unspecific dissociation rate constant or duration of sliding respectively has been discussed comprehensively in previous studies (16, 19, 21, 22, 28, 49). Here, we focused on how the search process adapts to promoters that involve co-activators and inhibitory competitors.

We considered the limit cases of exclusive dimerization in the nucleoplasm and exclusive dimerization on the target site in absence of a stabilizing protein-protein interaction (31). This allows direct comparison of search times and occupation frequencies of two coactivating TFs with a single TF. We found that two independently binding TFs prolong the target site search time significantly. Additionally, the unspecific dissociation rate constant μ_1 for an optimal target site search time increases. This increase is accompanied by a decrease of the transition rate constant μ_2 from a specifically to an unspecifically bound TF due to the law of detailed balance, meaning that the two TFs have to wait for each other in the specifically bound state to achieve fastest gene response times. Alternatively, dimeric TFs may wait for each other by increasing the specific dissociation rate constant μ . Whether dimeric TFs generally exhibit larger dissociation rate constants from unspecific DNA or smaller dissociation rate constants from specific target sites compared to solely activating TFs is subject to future studies.

For inducible dimers capable to dimerize in solution, the non-linear increase of target site search time at low dissociation rate constants may lead to a kinetic separation of monomer and dimer function. While uninduced monomers in principle could simultaneously arrive at the promoter, potentially evoking background activation, such a search mechanism is much slower than the one for dimer molecules that effectively bind as one TF. This turns background activation of uninduced monomeric molecules inefficient.

The occupation frequency of the promoter activated by two TFs drops significantly compared to the case of a single TF. The lower gene activation capability arises due to the more complex activation mechanism and could be accounted for by increasing the monomer concentration or by allowing dimerization not only on DNA but already in the nucleoplasm. This constitutes an additional advantage for solution-based dimerization and sheds new light on the question whether for example nuclear receptors bind to DNA as monomers or dimers (50).

We have discussed the influence of a competitor that inhibits binding to the specific target site, in addition to incorporating the effect of molecular crowding to the search process (20, 23-25, 48) by considering unspecific sites of fixed length mimicking static obstacles to sliding. The modulatory effect of an inhibitory competitor on the target site search time and occupation frequency of a TF can be mainly ascribed to blocking of the specific site rather than preventing the TF from scanning unspecific DNA sequences common to all DNA binding proteins. Thus, an inhibitory competitor will indeed only alter the activity of a certain gene without changing the search times or occupation frequencies of other genes.

When comparing our results to experimentally measured dissociation rate constants of eukaryotic TFs, we find that TFs indeed operate at the optimum of a fast target site search, but high occupation frequencies are not necessarily achieved in cells. While the low occupation frequency could in principle be counteracted by a high specific dissociation rate constant, such a strategy does not seem to occur for most TFs. A possible reason for suboptimal occupation frequency could arise from the stability paradox (16, 17), which states that the energy gap between unspecific and specific binding cannot be arbitrarily high and a compromise between both values might need to be attained. On the other hand, these particular choices of specific dissociation rate constants may also be advantageous for the functioning of TFs. Most eukaryotic TFs act not only on one promoter but regulate hundreds of genes and contribute to different signalling cascades. In such a genetic network short specific binding times ensure that always a large fraction of molecules is available in solution and the time to find a specific target site is kept low. This enables fast reactions to changing signalling environments. In contrast, the long specific binding time measured for the chromatin architecture protein CTCF (44) leads to a high fraction of occupied target sites and a considerable reduction of free protein. Thus, the target site search time is high once a CTCF molecule dissociated and CTCF-mediated chromatin loops will only reform slowly.

Optimizing for fast target site search and high occupation frequency may not be the only constraint in the evolution of dissociation rate constants. Given the complexity of gene regulation, target site search might not be the rate limiting step. Additionally, other requirements such as fast reaction to signals or a kinetic separation of monomer and dimer function may shape TF dissociation rate constants.

Acknowledgements

We thank Matthias Reisser for helpful discussions. This work was supported by the German Research Foundation [GE 2631/1-1 to J.C.M.G.] and the European Research Council (ERC) under the European Union's Horizon 2020 Research and Innovation Programme [637987 ChromArch to J.C.M.G.].

Author Contributions

J.H. and J.C.M.G. designed the study; J.H. performed calculations; J.H. and J.C.M.G. wrote the manuscript.

References

1. van Hijum, S., M. H. Medema, and O. P. Kuipers. 2009. Mechanisms and Evolution of Control Logic in Prokaryotic Transcriptional Regulation. *Microbiology and Molecular Biology Reviews* 73:481-+.
2. Venters, B. J., and B. F. Pugh. 2009. How eukaryotic genes are transcribed. *Critical Reviews in Biochemistry and Molecular Biology* 44:117-141.
3. Amoutzias, G. D., D. L. Robertson, Y. V. de Peer, and S. G. Oliver. 2008. Choose your partners: dimerization in eukaryotic transcription factors. *Trends in Biochemical Sciences* 33:220-229.
4. Horwitz, K. B., T. A. Jackson, D. L. Rain, J. K. Richer, G. S. Takimoto, and L. Tung. 1996. Nuclear receptor coactivators and corepressors. *Molecular Endocrinology* 10:1167-1177.
5. Coulon, A., C. C. Chow, R. H. Singer, and D. R. Larson. 2013. Eukaryotic transcriptional dynamics: from single molecules to cell populations. *Nature Reviews Genetics* 14:572-584.
6. Clauß, K., A. P. Popp, L. Schulze, J. Hettich, M. Reisser, L. Escoter Torres, N. H. Uhlenhaut, and J. C. M. Gebhardt. 2017. DNA residence time is a regulatory factor of transcription repression. *Nucleic Acids Research*.
7. Bain, D. L., Q. Yang, K. D. Connaghan, J. P. Robblee, M. T. Miura, G. D. Degala, J. R. Lambert, and N. K. Maluf. 2012. Glucocorticoid Receptor-DNA Interactions: Binding Energetics Are the Primary Determinant of Sequence-Specific Transcriptional Activity. *Journal of Molecular Biology* 422:18-32.
8. Winter, R. B., O. G. Berg, and P. H. Vonhippel. 1981. Diffusion-Driven Mechanisms Of Protein Translocation On Nucleic-Acids .3. The Escherichia-Coli-Lac Repressor-Operator Interaction - Kinetic Measurements And Conclusions. *Biochemistry* 20:6961-6977.
9. Berg, O. G., R. B. Winter, and P. H. Vonhippel. 1981. Diffusion-Driven Mechanisms Of Protein Translocation On Nucleic-Acids .1. Models And Theory. *Biochemistry* 20:6929-6948.
10. Kabata, H., O. Kurosawa, I. Arai, M. Washizu, S. A. Margarson, R. E. Glass, and N. Shimamoto. 1993. Visualization Of Single Molecules Of Rna-Polymerase Sliding Along Dna. *Science* 262:1561-1563.
11. Blainey, P. C., A. M. van Oijent, A. Banerjee, G. L. Verdine, and X. S. Xie. 2006. A base-excision DNA-repair protein finds intrahelical lesion bases by fast sliding in contact with DNA. *Proceedings of the National Academy of Sciences of the United States of America* 103:5752-5757.
12. Elf, J., G. W. Li, and X. S. Xie. 2007. Probing transcription factor dynamics at the single-molecule level in a living cell. *Science* 316:1191-1194.
13. Kim, J. H., and R. G. Larson. 2007. Single-molecule analysis of 1D diffusion and transcription elongation of T7 RNA polymerase along individual stretched DNA molecules. *Nucleic Acids Research* 35:3848-3858.
14. Gorman, J., A. J. Plys, M. L. Visnapuu, E. Alani, and E. C. Greene. 2010. Visualizing one-dimensional diffusion of eukaryotic DNA repair factors along a chromatin lattice. *Nature Structural & Molecular Biology* 17:932-U937.
15. Hammar, P., P. Leroy, A. Mahmutovic, E. G. Marklund, O. G. Berg, and J. Elf. 2012. The lac Repressor Displays Facilitated Diffusion in Living Cells. *Science* 336:1595-1598.
16. Gerland, U., J. D. Moroz, and T. Hwa. 2002. Physical constraints and functional characteristics of transcription factor-DNA interaction. *Proceedings of the National Academy of Sciences of the United States of America* 99:12015-12020.

17. Slutsky, M., and L. A. Mirny. 2004. Kinetics of protein-DNA interaction: Facilitated target location in sequence-dependent potential. *Biophysical Journal* 87:4021-4035.
18. Hu, T., A. Y. Grosberg, and B. I. Shklovskii. 2006. How proteins search for their specific sites on DNA: The role of DNA conformation. *Biophysical Journal* 90:2731-2744.
19. Klenin, K. V., H. Merlitz, J. Langowski, and C. X. Wu. 2006. Facilitated diffusion of DNA-binding proteins. *Physical Review Letters* 96.
20. Li, G. W., O. G. Berg, and J. Elf. 2009. Effects of macromolecular crowding and DNA looping on gene regulation kinetics. *Nature Physics* 5:294-297.
21. de la Rosa, M. A. D., E. F. Koslover, P. J. Mulligan, and A. J. Spakowitz. 2010. Dynamic Strategies for Target-Site Search by DNA-Binding Proteins. *Biophysical Journal* 98:2943-2953.
22. Bauer, M., and R. Metzler. 2012. Generalized Facilitated Diffusion Model for DNA-Binding Proteins with Search and Recognition States. *Biophysical Journal* 102:2321-2330.
23. Shvets, A. A., and A. B. Kolomeisky. 2016. Crowding on DNA in Protein Search for Targets. *Journal of Physical Chemistry Letters* 7:2502-2506.
24. Krepel, D., and Y. Levy. 2016. Protein diffusion along DNA: on the effect of roadblocks and crowders. *Journal of Physics a-Mathematical and Theoretical* 49.
25. Koslover, E. F., M. D. de la Rosa, and A. J. Spakowitz. 2017. Crowding and hopping in a protein's diffusive transport on DNA. *Journal of Physics a-Mathematical and Theoretical* 50.
26. Hippel, P. H. V., A. Revzin, C. A. Gross, and A. C. Wang. 1974. Non-specific DNA Binding of Genome Regulating Proteins as a Biological Control Mechanism: 1. The lac Operon: Equilibrium Aspects. *Proceedings of the National Academy of Sciences* 71:4808-4812.
27. Vonhippel, P. H., and O. G. Berg. 1986. ON THE SPECIFICITY OF DNA-PROTEIN INTERACTIONS. *Proceedings of the National Academy of Sciences of the United States of America* 83:1608-1612.
28. Mirny, L., M. Slutsky, Z. Wunderlich, A. Tafvizi, J. Leith, and A. Kosmrlj. 2009. How a protein searches for its site on DNA: the mechanism of facilitated diffusion. *Journal of Physics a-Mathematical and Theoretical* 42.
29. McGhee, J. D., and P. H. V. Hippel. 1974. Theoretical Aspects Of Dna-Protein Interactions - Cooperative And Non-Cooperative Binding Of Large Ligands To A One-Dimensional Homogeneous Lattice. *Journal of Molecular Biology* 86:469-489.
30. Van Kampen, N. G. 1992. Stochastic processes in physics and chemistry. Elsevier.
31. Gorman, J., and E. C. Greene. 2008. Visualizing one-dimensional diffusion of proteins along DNA. *Nature Structural & Molecular Biology* 15:768-774.
32. Mustonen, V., and M. Lassig. 2005. Evolutionary population genetics of promoters: Predicting binding sites and functional phylogenies. *Proceedings of the National Academy of Sciences of the United States of America* 102:15936-15941.
33. Halford, S. E., and J. F. Marko. 2004. How do site-specific DNA-binding proteins find their targets? *Nucleic Acids Research* 32:3040-3052.
34. Geisel, N., and U. Gerland. 2011. Physical Limits on Cooperative Protein-DNA Binding and the Kinetics of Combinatorial Transcription Regulation. *Biophysical Journal* 101:1569-1579.
35. Morisaki, T., W. G. Muller, N. Golob, D. Mazza, and J. G. McNally. 2014. Single-molecule analysis of transcription factor binding at transcription sites in live cells. *Nature Communications* 5.
36. Caccianini, L., D. Normanno, I. Izeddin, and M. Dahan. 2015. Single molecule study of non-specific binding kinetics of LacI in mammalian cells. *Faraday Discussions* 184:393-400.

37. Ball, D. A., G. D. Mehta, R. Salomon-Kent, D. Mazza, T. Morisaki, F. Mueller, J. G. McNally, and T. S. Karpova. 2016. Single molecule tracking of Ace1p in *Saccharomyces cerevisiae* defines a characteristic residence time for non-specific interactions of transcription factors with chromatin. *Nucleic Acids Research* 44.

38. Speil, J., E. Baumgart, J. P. Siebrasse, R. Veith, U. Vinkemeier, and U. Kubitscheck. 2011. Activated STAT1 Transcription Factors Conduct Distinct Saltatory Movements in the Cell Nucleus. *Biophysical Journal* 101:2592-2600.

39. Mazza, D., A. Abernathy, N. Golob, T. Morisaki, and J. G. McNally. 2012. A benchmark for chromatin binding measurements in live cells. *Nucleic Acids Research* 40.

40. Gebhardt, J. C. M., D. M. Suter, R. Roy, Z. Q. W. Zhao, A. R. Chapman, S. Basu, T. Maniatis, and X. S. Xie. 2013. Single-molecule imaging of transcription factor binding to DNA in live mammalian cells. *Nature Methods* 10:421-+.

41. Chen, J. J., Z. J. Zhang, L. Li, B. C. Chen, A. Revyakin, B. Hajj, W. Legant, M. Dahan, T. Lionnet, E. Betzig, R. Tjian, and Z. Liu. 2014. Single-Molecule Dynamics of Enhanceosome Assembly in Embryonic Stem Cells. *Cell* 156:1274-1285.

42. Hammar, P., M. Wallden, D. Fange, F. Persson, O. Baltekin, G. Ullman, P. Leroy, and J. Elf. 2014. Direct measurement of transcription factor dissociation excludes a simple operator occupancy model for gene regulation. *Nature Genetics* 46:405-+.

43. Sugo, N., M. Morimatsu, Y. Arai, Y. Kousoku, A. Ohkuni, T. Nomura, T. Yanagida, and N. Yamamoto. 2015. Single-Molecule Imaging Reveals Dynamics of CREB Transcription Factor Bound to Its Target Sequence. *Scientific Reports* 5:9.

44. Agarwal, H., M. Reisser, C. Wortmann, and J. C. M. Gebhardt. 2017. Direct Observation of Cell-Cycle-Dependent Interactions between CTCF and Chromatin. *Biophysical Journal* 112:2051-2055.

45. Geiger, T., A. Wehner, C. Schaab, J. Cox, and M. Mann. 2012. Comparative Proteomic Analysis of Eleven Common Cell Lines Reveals Ubiquitous but Varying Expression of Most Proteins. *Molecular & Cellular Proteomics* 11.

46. Nagaraj, N., J. R. Wisniewski, T. Geiger, J. Cox, M. Kircher, J. Kelso, S. Paabo, and M. Mann. 2011. Deep proteome and transcriptome mapping of a human cancer cell line. *Molecular Systems Biology* 7.

47. Kamar, R. I., E. J. Banigan, A. Erbas, R. D. Giuntoli, M. O. de la Cruz, R. C. Johnson, and J. F. Marko. 2017. Facilitated dissociation of transcription factors from single DNA binding sites. *Proceedings of the National Academy of Sciences of the United States of America* 114:E3251-E3257.

48. Morelli, M. J., R. J. Allen, and P. R. ten Wolde. 2011. Effects of Macromolecular Crowding on Genetic Networks. *Biophysical Journal* 101:2882-2891.

49. Von Hippel, P. H., and O. G. Berg. 1989. Facilitated Target Location In Biological-Systems. *Journal of Biological Chemistry* 264:675-678.

50. Ong, K. M., J. A. Blackford, Jr., B. L. Kagan, S. S. Simons, Jr., and C. C. Chow. 2010. A theoretical framework for gene induction and experimental comparisons. *Proceedings of the National Academy of Sciences of the United States of America* 107:7107-7112